AD-A151 760 HIGH GAIN XUV AND X-RAY FREE ELECTRON LASERS(U) NAVAL RESEARCH LAB WASHINGTON DC C M TANG ET AL. 1984 1/1

UNCLASSIFIED F/G 20/5 NL

END

FILMED

DTIC

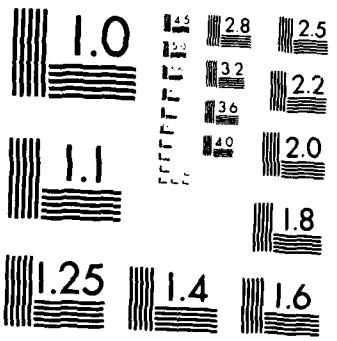

Submitted to: Free Electron Generation of Extreme Ultraviolet Coherent Radiation, AIP Conf. Proc. No. 118, (ed. J.M.J. Madey & C. Pellegrini), p. 131 (1984)

HIGH GAIN XUV AND X-RAY FREE ELECTRON LASERS

C. M. Tang and P. Sprangle
U. S. Naval Research Laboratory, Washington, D. C. 20375

ABSTRACT

The operation of the free electron laser (FEL) oscillator in the XUV and X-ray regimes requires high gain per pass to overcome somewhat large mirror losses. This paper summarizes the growth rates and intrinsic trapping efficiencies in the high gain regimes, and comments on various three-dimensional effects.

INTRODUCTION

Operation of the free electron laser oscillator at ultraviolet (UV) frequencies[1] has been demonstrated utilizing a storage ring. By employing the planned Stanford University storage ring[2], FEL operations at XUV and X-ray frequencies seem feasible. The future trend in the production of XUV and X-ray FELs is toward long wigglers, operating in the high gain, i.e., exponential growth regime, in an oscillator configuration. This paper will address the physics in the high gain regime[3-9] and the modeling of three-dimensional (3-D) effects relevant to FEL oscillators.

FEL OPERATING REGIMES

Characteristics of electron beam sources divide the FEL interaction mechanism into four major categories: i) low gain, single particle regime, ii) high gain, cold beam, single particle regime, iii) high gain, warm beam , single particle regime, and iv) high gain, cold beam, collective regime. XUV and X-ray FELs necessarily must operate in a high gain regime because available mirrors are somewhat lossy. The properties of each of the operating FEL regimes or categories are summarized below.

i) Low Gain, Single Particle, Cold Beam Regime

FELs utilizing electron beams with the characteristics of high energy, low current, and high quality (low emittance), operate in the low gain, Compton regime. The interaction physics is primarily governed by single particle effects, i.e., collective or space charge effects can be neglected. In the low gain limit, the total amplitude gain of the radiation field is on the order of unity or less, i.e., $g \lesssim 1$, where

$$g \simeq 2\pi F \zeta N^3 \qquad (1)$$

is the maximum amplitude gain per pass, where

$$\zeta = \frac{\pi}{\sigma_b} \frac{I}{I_A} \gamma \lambda^2 \frac{K^2}{(1 + K^2)^2}, \qquad (2)$$

I/I_A is the Budker's parameter, I is the total beam current in amperes, $I_A = 17\times10^3$ A is the Alfven current, σ_b is the cross sectional area of the electron beam, λ is the wavelength of the radiation, γ is the total relativistic energy factor, N is the number of wiggler periods, $K = (|e|/m_o c^2) \langle A_W \rangle_{RMS}$ is the RMS wiggler parameter and A_W is the vector potential of the wiggler. The numerical value of ζ is typically much less than unity.

We included a filling factor, F, in the expressions for the gain. The filling factor is defined as $0 < F = \Sigma_b/\sigma_R < 1$, where σ_R is the cross sectional area of the radiation, and Σ_b is the cross sectional area of the electron beam that overlaps the radiation beam.

The efficiency is defined as $\eta = (P_L - P_i)/P_e$, where P_L is the laser power at the exit of the wiggler, P_i is the laser power at the entrance of the wiggler, and P_e is the power in the electron beam. The efficiency in the low gain limit is

$$\eta = f/2N, \qquad (3)$$

where $f = \Sigma_b/\sigma_b < 1$ is the filling factor for the efficiency.

ii) <u>High Gain, Single Particle, Cold Beam Limit</u>

The high gain limit implies exponential growth of the radiation in the FEL interaction region. Here the wavenumber k in the dispersion relation describing the interaction acquires an imaginary component such that $-\int_0^{L_w} \mathrm{Im}(k)dz >> 1$, where L_w is the length of the wiggler and Im(k) denotes the imaginary part of k. In the high gain limit, the FEL is said to be in the single particle regime if the ponderomotive potential dominates the space charge potential. When the reverse is true, the FEL is said to be in the collective (Raman) regime. The criteria for the FEL to be in the single particle high gain regime[5-7] is

$$\zeta << 0.01 \left(\frac{K^2}{1 + K^2}\right)^3. \qquad (4)$$

When the energy spread of the electron beam satisfies

$$\frac{\Delta\gamma}{\gamma} \lesssim 0.15\ \zeta^{1/3}, \tag{5}$$

the electron beam can be considered cold and the ponderomotive potential wave interacts strongly with all the electrons. The maximum number of e-folds for the radiation amplitude obtained from the dispersion relation[4-7,9] is

$$\alpha = 3.2\ F^{1/3}\ \zeta^{1/3}\ N. \tag{6}$$

The intrinsic trapped particle efficiency at the maximum growth rate[5-7] is

$$\eta = 0.29\ f\ \zeta^{1/3}. \tag{7}$$

iii) High Gain, Single Particle, Warm Beam Limit

When the energy spread of the electron beam is large, the ponderomotive wave interacts strongly with only a small fraction of the thermal electrons. The growth rate and efficiences can be significantly reduced from the cold beam limit. The maximum number of e-folds in the wiggler length[4-5] is

$$\alpha = 0.23\ F\ \zeta\ N\ \left(\frac{\gamma}{\Delta\gamma}\right)^2, \tag{8}$$

and the corresponding efficiency[5] is

$$\eta = 4.6\times10^{-6}\ f\ \zeta^3\ \left(\frac{\gamma}{\Delta\gamma}\right)^8. \tag{9}$$

iv) High Gain, Collective, Cold Beam Limit

The FEL is in the collective regime when the space charge potential becomes comparable to or larger than the ponderomotive potential. The space charge potential enhances the growth rate[3-7]. The maximum number of e-folds in the wiggler is

$$\alpha = (2\pi\ F)^{1/2}\left(\zeta\ \frac{K^2}{1+K^2}\right)^{1/4} N, \tag{10}$$

and the efficiency at maximum growth rate[3,5-7] is,

$$\eta = \frac{2}{\pi}\left(\zeta\ \frac{1+K^2}{K^2}\right)^{1/2}. \tag{11}$$

The relevant formulas are summarized in Table I. Note that the gain and the number of e-folds are proportional to different powers of the filling factor depending on the FEL regime. In the high gain regimes, the efficiencies are independent of the number of the wiggler periods, while the number of e-folds α are proportional to the number of wiggler periods, N. This is in contrast to the low gain regime.

EXAMPLE

To illustrate the high gain limit, we will consider an example based on the parameters of the Stanford storage ring, and a laser radiation wavelength of 200Å. The relevant parameters are given in Table II. The dispersion relation[4-7] for the high gain, cold beam, single particle regime as well as the high gain, cold beam, collective regime is

$$\delta k \left(\delta k + \frac{4}{\pi} \left(\frac{1 + K^2}{K^2} \zeta\right)^{1/2}\right) \left(\delta k + \frac{\Delta\omega}{\omega_o}\right) = - \mu^2, \qquad (12)$$

where $k/k_w = 2\gamma^2(1 + K^2)^{-1}(\omega/\omega_o) - (2/\pi)\ (\zeta\ (1 + K^2)^2/K^2)^{1/2} + \delta k$ is the normalized wavenumber, $\mu^2 = 2\ F\ \zeta\ (1 + K^2)^2/(\lambda^2\ \gamma^4)$, $\Delta\omega = \omega - \omega_o$, and $\omega_o = 2\gamma^2(1 + K^2)^{-1}\ k_w c$ is the resonant frequency, $k_w = 2\pi/\ell_w$ is the wavenumber of the wiggler, and ℓ_w is the wavelength. The growth rate is given by

$$\Gamma = - \mathrm{Im}(\delta k)\ k_w. \qquad (13)$$

The number of e-folds α within the wiggler, i.e., $I_w\Gamma$, is

$$\alpha = - 2\pi N\ \mathrm{Im}(\delta k). \qquad (14)$$

The expression for the efficiency[5-7] is

$$\eta = f\ \left[\frac{2}{\pi} \left(\frac{1 + K^2}{K^2}\ \zeta\right)^{1/2} + \mathrm{Re}(\delta k)\right]. \qquad (15)$$

The trapped particle saturated radiation field (normalized vector potential) expressed in terms of the efficiency in the high gain limit is

$$a_{trap} = \frac{1}{\pi} \left[\zeta\ \eta\ \frac{(1 + K^2)^2}{K^2}\right]^{1/2}. \qquad (16)$$

Table I. Summary of the FEL Regimes

FEL Operating Regime	Operating Criteria	Max. Amplitude gain, g, or Max. No. of e-folds, α	Trapped Particle Power Efficiency, η, at Peak Gain
Low Gain - Compton (cold beam)	$g \lesssim 1$ $\Delta\gamma/\gamma \ll 1/2N$	$g = 2\pi F \zeta N^3$	$f/2N$
High Gain (cold beam) (single particle)	$\alpha \gg 1$ $\Delta\gamma/\gamma \ll 0.15\,\zeta^{1/3}$ $\zeta \ll 0.01\,K^6 (1+K^2)^{-3}$	$\alpha = 3.2\,F^{1/3}\,\zeta^{1/3}\,N$	$0.29\,f\,\zeta^{1/3}$
High Gain (warm beam) (single particle)	$\alpha \gg 1$ $\Delta\gamma/\gamma \gtrsim 0.15\,\zeta^{1/3}$ $\zeta \ll 0.01\,K^6 (1+K^2)^{-3}$	$\alpha = 0.23\,F\,\zeta\,N\,(\frac{\gamma}{\Delta\gamma})^2$	$4.6\times10^{-6}\,f\,\zeta^3\,(\frac{\gamma}{\Delta\gamma})^8$
High Gain (collective) (cold beam)	$\alpha \gg 1$ $\Delta\gamma/\gamma \ll \eta/2$ $\zeta \gtrsim 0.01\,K^6 (1+K^2)^{-3}$	$\alpha = (2\pi F)^{1/2}(\zeta \frac{K^2}{1+K^2})^{1/4} N$	$\frac{2}{\pi} f (\zeta \frac{1+K^2}{K^2})^{1/2}$

where $\zeta = (\pi/\sigma_b)\,(I/I_A)\,\gamma\,\lambda^2K^2(1+K^2)^{-2}$, I/I_A is the Budker's parameter, I is the total beam current in amperes, $I_A = 17\times10^3$A is the Alfven current, σ_b is the area of the electron beam, λ is the wavelength of the radiation, γ is the relativistic energy factor, K is the wiggler parameter, and $F = \Sigma_b/\sigma_R$ is the filling factor for the gain or growth rate, σ_R is the area of the radiation beam, Σ_b is the area of the electron beam that overlaps the radiation beam, and $f = \Sigma_b/\sigma_b$ is a filling factor for the efficiency coefficient.

Table II: 200 Å FEL using the Stanford Storage Ring Parameters

FEL Parameters	
wiggler length, L_w	20 m
wiggler period, ℓ_w	5.42 cm
wiggler parameter, K	1.4
number of wiggler periods, N	369
energy of the electron beam, E	1 GeV
peak current, I	100 A - 270 A
electron beam radius, r_b	125 μm
radiation wavelength, λ	200 Å
minimum radiation waist, w_o	192 μm
filling factor, $F = 2r_b^2/w_o^2$	0.8
mirror losses, L_s	75%

Calculated Parameters for High Gain Cold Beam Limit with I = 100 A Peak	
Budker's parameter, I/I_A	5.88×10^{-3}
maximum allowable $\Delta\gamma/\gamma$	0.06%
ζ	6.73×10^{-8}
maximum number of e-folds, α (F = 0.8)	4.5
efficiency at maximum gain, η	0.12%

Calculated Parameters for High Gain Cold Beam Limit with I = 270 A Peak	
Budker's parameter, I/I_A	1.59×10^{-2}
maximum allowable, $\Delta\gamma/\gamma$	0.09%
ζ	1.82×10^{-7}
maximum number of e-folds, α (F = 0.8)	6.2
efficiency at maximum gain, η	0.17%

The dispersion relation (12) is solved numerically for a range of frequencies. Plots of the growth rate Γ and the number of e-folds α versus the frequency mismatch parameter ν are shown in Fig. 1 for I = 100 A and 270 A, where the frequency mismatch parameter is defined in the conventional way, $\nu = -\pi N \frac{\Delta\omega}{\omega_o}$. The maximum growth rate is at $\nu = 0$. The dashed curve in Fig. 1 is computed with the lower peak current; it has a smaller growth rate and a reduced bandwidth. The actual number of e-folds would be reduced by about one from the value given in Fig. 1 due to launching losses.

The corresponding trapped particle efficiencies are plotted in Fig. 2. The efficiencies at $\nu = 0$ are 0.12% and 0.17% for I = 100 A and I = 270 A, respectively. The efficiencies increase as ν increases. Even though the growth rate spectrum is wide, the useful bandwidth is actually small, due to the falloff in efficiency.

OSCILLATOR CONSIDERATIONS

FELs in the XUV and X-ray regimes are expected to operate in an oscillator configuration. The oscillator reaches a steady state when

$$G = L_s/(1 - L_s), \tag{17}$$

and

$$P_i = \frac{\eta^*}{G} P_e, \tag{18}$$

where η^* is the actual efficiency at saturation, L_s is the power loss, and $G = (P_L - P_i)/P_i$ is the power gain. The laser power produced per turn is $G\,P_i$. If the electron beam source is not a recirculating beam, then the laser saturates by trapping the electrons and the efficiency η^* is given in Table I.

When the electron beam from a storage ring is radiating in steady state, the FEL most likely would operate in the high gain, thermal beam, single particle regime. Here, the electron energy spread increases, while the gain decreases until $G = L_s/(1 - L_s)$. The limit on the energy spread is

$$\frac{\Delta\gamma}{\gamma} = [0.23\, F\, \zeta\, N/\alpha_m]^{1/2}, \tag{19}$$

where $\alpha_m = \ln(G + 1)/2 + 1$ is the minimum required number of e-folds. The addition of one e-fold is to compensate for the launching loss[6-9]. The efficiency and radiated power of the FEL in the storage ring is constrained by the Renieri limit[10-11]. In

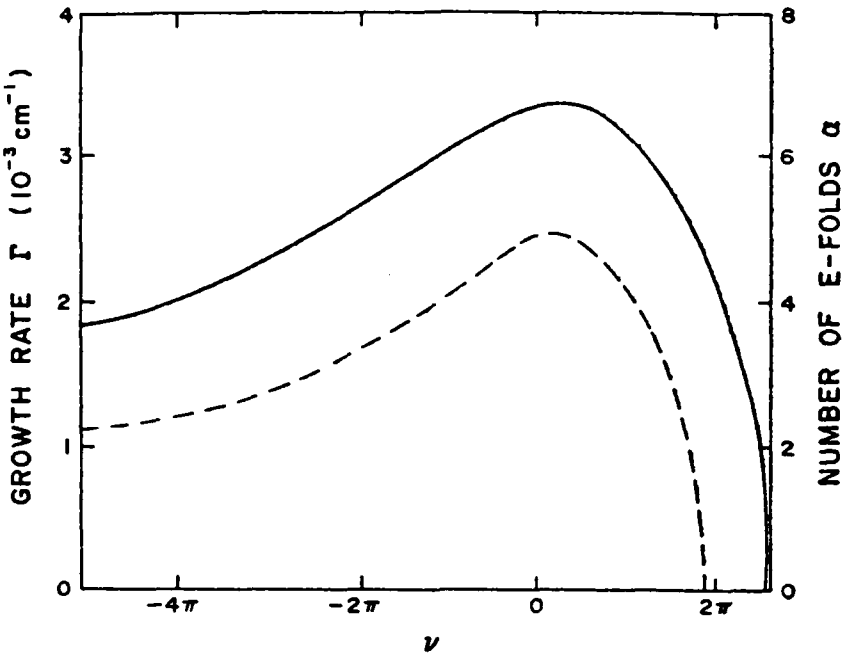

Fig. 1 Plots of growth rate Γ and number of e-folds α versus frequency mismatch parameter ν for I = 100 A (- -) and I = 270 A (——). We have taken F = 1 here.

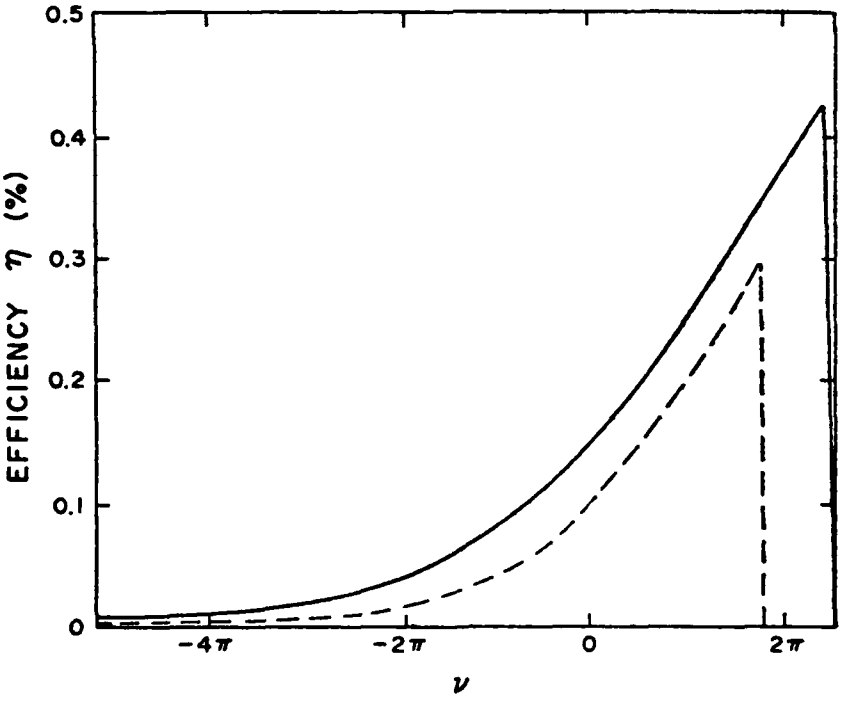

Fig. 2 Plots of the intrinsic trapping efficiency η versus frequency mismatch parameter ν for I = 100 A (- -) and I = 270 A (——). We have taken f = 1 here.

the low gain case, the actual efficiency $\eta^* \lesssim (2N)^{-1}(P_s/P_e)$ is much less than the trapping efficiency $1/2N$, where P_s is the power of the synchrotron emission. Even though a comprehensive analysis has yet to be carried out for a high gain FEL with thermal beam in a storage ring, the actual efficiency η^* is expected to be very low. If $\eta^* = \eta_{th}$, the FEL saturates by trapping in the warm beam limit, where η_{th} is the trapping efficiency which can be expressed in terms of the minimum required number of e-folds α_m

$$\eta_{th} = 1.6\times10^{-3}\left(\frac{\alpha_m}{FN}\right)^4 \frac{f}{\zeta} . \qquad (20)$$

If $\eta^* < \eta_{th}$, the FEL oscillator reaches a steady state without trapping the electrons.

COMMENTS ON 3-D EFFECTS

The 3-dimensional effects come into the problem because of: 1) finite beam emittance, 2) transverse gradient in the magnetic wiggler, 3) transverse radiation profile, and 4) axial variation of the radiation pulse. Based on the bench mark example in Table II, we will eliminate the 3-D effects which are not important and suggest an appropriate 3-D radiation propagation model.

The first 3-D effect that we consider is due to the transverse gradient in the magnetic wiggler, resulting in betatron oscillations[12-14]. The betatron wavenumber for the linearly polarized wiggler is $k_\beta = K\, k_w/\gamma = 8.1\times10^{-4}$ cm^{-1}. In our example, the betatron wavelength $L_\beta = 2\pi/k_\beta$ is 77 m. Since $L_\beta \gg L_w$ the effect of betatron oscillations on the particle trajectory is not very significant. To maintain the e-beam radius roughly constant in the wiggler, the radius at the entrance of the wiggler should satisfy

$$r_b = \left(\frac{\varepsilon}{\pi k_\beta}\right)^{1/2}. \qquad (21)$$

Betatron oscillations are a source of energy spread. For r_b = 125 μm, the effective energy spread $\Delta E_\beta/E$ due to the betatron oscillations is much smaller than the imposed limit on $\Delta\gamma/\gamma$.

Recently, M. Rosenbluth pointed out that betatron oscillations are capable of causing particle detrapping in the ponderomotive potential well formed by the 3-D radiation field and the wiggler field[15]. Detrapping becomes an important issue when twice the betatron oscillation frequency is roughly equal to the

synchrotron frequency in the ponderomotive potential well. This instability will occur when all of the following criteria are satisfied:

i) The FEL reaches saturation. In the linear growth regime of the high gain FEL, the synchrotron frequencies are continuously changing so that resonance cannot be established.

ii) It is required that $2k_\beta \sim \Omega$, where

$$\Omega = 2\, k_w \left(\frac{K}{1 + K^2}\, a_R\right)^{1/2}, \tag{22}$$

is the synchrotron wavenumber, $a_R = (|e|/m_o c^2)\langle A_R\rangle_{RMS}$ is the normalized vector potential of the radiation field. The appropriate value for the actual amplitude of the radiation vector potential A_R is that at saturation.

iii) The length of the wiggler is long enough for the instability to grow, i.e., $L_w \gtrsim L_\beta$. The FEL under consideration is not likely to satisfy all of the above criteria.

Next, we consider the axial variations of the radiation pulse. These effects can be grouped into two categories: i) variations of the length scale on the order of the electron pulse length ℓ_{eb}, and ii) length scale variation on the order of the pulse slippage distance $s = N\lambda$. The long spatial scale variation is controlled by mirror detuning distance, while the short scale variation is controlled by trapped particle instabilities.

When the source of the electron beam is from a storage ring, the length of the electron pulse is much longer than the pulse slippage distance. In this case, the mirror detuning distance δL_m is not as critical as when the electron pulse length is comparable to the pulse slippage distance, where $\delta L_m = 2L_m/c - L/v_o$, L_m is the separation of the mirrors, L is the distance separating two electron pulses and $v_o = c(1 - 1/\gamma^2)^{1/2}$. When the mirror detuning length is 0, the length of the radiation pulse would be on the order of the length of the electron pulse. In a high gain lossy FEL oscillator, the steady state radiation pulse length decreases as the detuning length $|\delta L_m|$ increases.

The axial pulse structure would be smooth if the snychrotron oscillation of the electrons in the ponderomotive potential well does not result in the growth of sideband frequencies[16-20]. Numerical simulations of the FEL oscillator in the low gain regime[18,20] showed that the period of the amplitude modulation $\bar{\lambda}$ due to sidebands is roughly equal to the pulse slippage distance $s = N\lambda$. The frequency of the sidebands are at $\omega_o \pm \delta\omega$, and $\delta\omega \simeq \omega_o/N$, or $\delta\nu \simeq \pi$. The sidebands grow when the period of the synchrotron oscillation is roughly the length of the wiggler. Therefore, the required RMS radiation vector potential for the growth of the side band frequency is

$$a_R = \frac{1}{4\,N^2}\,\frac{(1+K^2)^2}{K^2}. \tag{23}$$

The corresponding required radiation power for the sideband instabilities to occur in the low gain limit is

$$P_L = \frac{c\,w_o^2}{8}\left(\frac{2\pi}{\lambda}\,\frac{m_o c^2}{|e|}\,a_R\right)^2, \tag{24}$$

where w_o is the minimum waist of the radiation.

In the high gain oscillator, the criteria for sideband growth are slightly different. The first requirement is that the electrons reach the trapped particle saturation regime. If the electrons are trapped, the sideband frequencies occur at

$$\delta\omega = \pm\,\frac{2\,\gamma^2}{1+K^2}\;c\,\Omega, \tag{25}$$

where Ω is the synchrotron wavenumber from Eq. (22). The appropriate amplitude of the radiation vector potential to be used in Ω is given by the trapped particle saturation field in Eq. (16). Finally it is required that the gain at the sideband frequencies be larger than the loss at saturation. In the high gain FEL, the period of the amplitude modulation $\bar{\lambda}$ is expected to be a function of the trapped particle efficiency and independent of the pulse slippage distance.

For FELs utilizing a storage ring electron beam, it is unlikely that sidebands would appear, since the above requirements appear difficult to satisfy. For FELs utilizing RF linacs, however, sideband growth could become a problem.

The growth of sidebands is not desirable for most applications. If sidebands do appear, they can be eliminated by the introduction of mirror loss, which will reduce the radiation power. Another method is to introduce frequency filtering. The optics in the frequency of interest naturally provide frequency filtering. The interference (multilayer) optics[21] for XUV has a band spectrum of $\Delta\lambda/\lambda \sim 10^{-1}$. Crystal Optics[21] for the X-ray regime has a band spectrum of $\Delta\lambda/\lambda \sim 10^{-5}$. For our example, we require $\Delta\lambda/\lambda \sim 2 \times 10^{-3}$.

The 3-D effect associated with the growth of radiation in the transverse direction for an electron beam radius comparable or larger than the minimum optical waist would have to be evaluated numerically. It is important to include the appropriate amount of energy spread in the model. If the sideband oscillations are important, 3-D pulse propagation calculation is necessary. The appropriate scheme is outlined in Refs. 19-20. If the sideband

oscillations are not important, one can perform a single frequency, 3-D wave propagation calculation using a variety of numerical schemes outlined in Refs. 22-26.

In conclusion, we believe that the effects associated with betatron oscillations in the wiggler and the sideband instabilities probably are not important transverse effects for XUV and X-ray FELs. The relevant transverse effects are energy spread and finite emittance of the electron beam in a 3-D radiation field.

ACKNOWLEDGMENT

This work was supported by DARPA under Contract No. 3817.

REFERENCES

1. P. Elleaume, presented at the 1983 FEL Workshop at Orcas Island, WA, Jun 26-Jul 1, 1983.
2. J. M. J. Madey, presented at the Free Electron Generation of Extreme Ultraviolet Coherent Radiation, Brookhaven National Lab., Upton, NY, Sep 19-22, 1983.
3. T. Kwan, J. M. Dawson and A. T. Lin, Phys. Fluids 20, 581 (1977).
4. N. M. Kroll and W. A. McMullin, Phys. Rev. A17, 300 (1978).
5. P. Sprangle, R. A. Smith and V. L. Granatstein, Infrared and Millimeter Waves, edited by K. Button, (Academic Press, New York, 1979), Vol. I.
6. P. Sprangle, C. M. Tang and W. M. Manheimer, Phys. Rev. A21, 302 (1980).
7. P. Sprangle and R. A. Smith, Phys. Rev. A21, 293 (1980).
8. C. M. Tang and P. Sprangle, J. Appl. Phys. 52, 3148 (1981).
9. C. Pellegrini, presented at the Free Electron Generation of Extreme Ultraviolet Coherent Radiation, Brookhaven National Lab, Upton, NY, Sep 19-22, 1983.
10. A. Renieri, IEEE Trans. Nucl. Sci. NS-26, 3827 (1979).
11. G. Dattoli and A. Renieri, "Experimental and Theoretical Aspects of the Free Electron Laser", submitted for publication 1983.
12. C. M. Tang and P. Sprangle, Phys. of Quantum Electronics, Vol. 7, 627 (1982)
13. T. L. Smith and J. M. J. Madey, Appl. Phys. B27, 195 (1982).
14. C. M. Tang, Proc. of the Int'l Conf. on Lasers '82, edited by R. Powell, (STS Press, McLean, VA, 1982), p. 164.
15. M. N. Rosenbluth, "Two-Dimensional Effects in FEL's" paper No. I-ARA-83-U-45 (ARA-488), Austin Research Assoc., Austin, TX, 1983.
16. N. M. Kroll and M. N. Rosenbluth, Physics of Quantum Electronics, Vol. 7, 147 (1980).
17. H. P. Freund, P. Sprangle and C. M. Tang, Phys. Rev. A25, 3121 (1982).

18. J. C. Goldstein and W. B. Colson, Proc. of the Int'l Conf. on Lasers '82, edited by R. Powell, (STS Press, McLean, VA, 1982), p. 218.
19. C. M. Tang and P. Sprangle, Proc. of the Int'l Conf. on Lasers '82, edited by R. Powell, (STS Press, McLean, VA, 1982), p. 177.
20. C. M. Tang and P. Sprangle, "Semi-Analytical Formulation of the Two-Dimensional Pulse Propagation in the Free Electron Laser Oscillator", to be published in the Proc. of the 1983 Free Electron Laser Workshop, held at Orcas Island, WA, Jun 26 - Jul 1, 1983.
21. D. Attwood, presented at the Free Electron Generation of Extreme Ultraviolet Coherent Radiation, Brookhaven National Lab., Upton, NY, Sep 19-22, 1983.
22. W. B. Colson and J. L. Richardson, Phys. Rev. Lett. 50, 1050 (1983).
23. D. Quimby and J. Slator, IEEE J. of Quantum Electron QE19, 800 (1983).
24. D. Prosnitz, R. A. Hass, S. Doss and R. J. Gelinas, Phys. of Quantum Electronics, Vol. 9, 1047 (1982).
25. C. J. Elliott, Proc. of the Bendor Free Electron Laser Conf. Held at Bendor, France, 26 Sep - 1 Oct, 1982, Journal de Physique, Tome 44, C1-255 (1983).
26. P. Elleaume and D. A. G. Deacon, "Transverse Mode Dynamics in a Free Electron Laser", submitted for publication 1983.

END

FILMED

5-85

DTIC